



## Technical note: Enhancement of float-pH data quality control methods: A study case in the Subpolar Northwest Atlantic region

Cathy Wimart-Rousseau<sup>1</sup>, Tobias Steinhoff<sup>1</sup>, Birgit Klein<sup>3</sup>, Henry Bittig<sup>4</sup>, and Arne Körtzinger<sup>1,2</sup>

<sup>1</sup>GEOMAR Helmholtz Centre for Ocean Research Kiel, Kiel, Germany

<sup>2</sup>Kiel University, Kiel, Germany

<sup>3</sup>Federal Maritime and Hydrographic Agency (BSH), Hamburg, Germany

<sup>4</sup>Leibniz Institute for Baltic Sea Research Warnemuende (IOW), Seestr. 15, 18119 Rostock, Germany

**Correspondence:** Cathy Wimart-Rousseau (cwimart-rousseau@geomar.de)

**Abstract.** Since a pH sensor has become available that is suitable for this demanding autonomous measurement platform, the marine CO<sub>2</sub> system can be observed independently and continuously by BGC-Argo floats. This opens the possibility to detect variability and long-term changes in interior ocean inorganic carbon storage and quantify the ocean sink for atmospheric CO<sub>2</sub>. In combination with a second parameter of the marine CO<sub>2</sub> system, pH can be a useful tool to derive the surface ocean CO<sub>2</sub> partial pressure (*p*CO<sub>2</sub>).

The large spatiotemporal variability of the marine CO<sub>2</sub> system requires sustained observations to decipher trends and punctual events (e.g., river discharge, phytoplankton bloom) but also puts a high emphasis on the quality control of float-based pH measurements. In consequence, as the interpretation of changes depends on accurate data, and because sensor offsets or drifts might appear, a consistent and rigorous correction procedure to process and quality-control the data has been established. By applying standardized routines of the Argo data management to pH measurements from a pH/O<sub>2</sub> float pilot array in the subpolar North Atlantic Ocean, we investigate the uncertainties and lack of objective criteria associated with the standardized routines, notably the choice of the reference method for the pH correction (CANYON-B or LIRPH) as well the reference depth for this correction. For the studied float array, significant differences of ca. 0.02 pH units are observed between the two reference methods which can be used to correct float-pH data from water samples. Through comparison against discrete pH data from water samples, an assessment of the adjusted float-pH data quality is presented. The results point out noticeable discrepancies near the surface of > 0.01 pH units. In the context of converting surface ocean pH measurements into *p*CO<sub>2</sub> data for the purpose to derive air-sea CO<sub>2</sub> fluxes, we conclude that the minimum accuracy requirement of 0.01 pH units (equivalent to the minimum *p*CO<sub>2</sub> accuracy of 10 μatm for potential future inclusion into the SOCAT database) is not systematically achieved in the upper ocean.

While the limited dataset and regional focus of our study provides only one showcase, it still calls for an additional independent pH reference in the surface ocean. We therefore propose a way forward to enhance the float-pH quality control procedure. In our analysis, the current philosophy of pH data correction against climatological reference data at one single depth in the deep ocean appears insufficient to assure adequate data quality in the surface ocean. Ideally, an additional reference point should be taken at or near the surface where the resulting *p*CO<sub>2</sub> data are of the highest importance to monitor the air-sea exchange of CO<sub>2</sub> and would have the potential to very significantly augment the impact of the current observation network.



## 1 Introduction

Since the beginning of the industrial era, the ocean has played a critical role by absorbing about 25% (Friedlingstein et al., 2022) of the annual anthropogenic CO<sub>2</sub> emissions, thereby mitigating the current climate change (IPCC, 2021). Ocean CO<sub>2</sub> uptake causes changes in the ocean chemistry, inducing an increase in hydronium ion concentration (i.e., a decrease in oceanic pH). Throughout the world ocean, these changes, also termed “ocean acidification” (OA; Doney et al., 2009), are already observed and a global surface ocean pH decline of 0.1 units since the beginning of the industrial era has been reported (Orr et al., 2005). Depending on emission scenarios, seawater will continue to become less alkaline with a projected pH decline ranging from 0.16 to 0.44 pH units by 2100 (e.g., Kwiatkowski et al., 2020). These changes, while being variable regionally and along the water column (Carstensen and Duarte, 2019; Orr et al., 2005), represent a significant environmental change and potential threat to marine organisms and marine ecosystems that needs to be elucidated.

To assess long-term changes in ocean chemistry, oceanographic cruises were conducted and discrete water samples were collected. These historical hydrographic data have been synthesized in databases such as the Global Ocean Data Analysis Project (GLODAPv2) database (Olsen et al., 2016) which provides an internally consistent reference data product. However, in addition to anthropogenic modifications, oceanic pH is a dynamic variable in response to biological, physical, and chemical processes and changes on daily to centennial timescales, with pronounced seasonal, interannual, and decadal variability. In consequence, ship-based observing strategies, being skewed towards certain months and regions, especially in some places where current sampling methods are not possible (e.g., permanently or seasonally ice-covered regions), cannot adequately capture the dynamic spatiotemporal variability of the carbonate system parameter.

In order to improve our understanding of the oceanic CO<sub>2</sub> cycle and to decipher any temporal change, sustained time-series measurements at fixed stations have been carried out over the last decades (e.g., Bates et al., 2014). Nevertheless, the low spatial coverage associated with these sampling sites, generally located near coastal areas, precludes a rigorous description of the open-ocean variability. Thus, these long-term data collections, with uneven regional distribution and typically moderate temporal resolutions (i.e., bi-weekly or monthly), lead to “observational gaps” with an under-sampling of biogeochemical variables (Tanhua et al., 2019).

To circumvent these gaps and overcome the existing severe limitations in terms of both spatial and temporal resolution, autonomous platforms such as moorings, profiling floats, underwater gliders, or surface vehicles have been deployed at a global scale (Bushinsky et al., 2019; Whitt et al., 2020) and contributed to the extension of databases (Abram et al., 2019). Recently, the development of a pH sensor suitable for deployment on autonomous platforms has extended our observation capabilities ability of the marine CO<sub>2</sub> system (Johnson et al., 2016).

Defined as an Essential Ocean Variable (EOV) by the Global Ocean Observing System (GOOS, [www.goosocean.org](http://www.goosocean.org)), pH can be used to determine marine CO<sub>2</sub> system changes in response to anthropogenic impacts. However, the key to this autonomous platform expansion is the achievable and documented quality of the pH data which relies on defined practices ranging from rigorous pre-deployment sensor calibration to post-deployment assurance of data accuracy and consistency (Johnson et al., 2018). Indeed, for reliably identifying and interpreting changes accurate and consistent data are needed.



60 For BGC-Argo floats data, operational procedures for physical data (temperature, salinity, pressure) qualification have been established, ranging from automated “Real-Time” (RT) checks to sophisticated “Delayed-Mode” (DM) adjustment (Schmechtig et al., 2016; Wong et al., 2022). For pH, numerous delayed-mode procedures have been suggested, but a uniform, fully tested and globally-proven correction method is still missing. Recently, in the framework of the Southern Ocean Carbon and Climate Observations and Modelling project (SOCCOM; Russell et al., 2014), a methodology has been developed to correct nitrate, pH, and oxygen values from sensor drifts and offsets in DM. Two Matlab tools named SAGE (SOCCOM Assessment and Graphical Evaluation) and SAGE-O2 have been created as interfaces to support the validation and correction of float pH and oxygen data, respectively. In the SAGE procedure (Maurer et al., 2021), the machine learning method ‘Carbonate system and Nutrient concentration from hYdrological properties and Oxygen, Bayesian approach’ (CANYON-B; Bittig et al., 2018b), the Locally Interpolated Regression (LIR) algorithmic methods (Carter et al., 2018) and multiple linear regression techniques (Williams et al., 2016) are used as a reference to correct float pH data at depths of typically around 1500 dbar. The neural-network CANYON-B approach is based on the approach originally developed by (Sauzède et al., 2017).

We have applied the SAGE tool and the included correction methods on float pH data acquired from a pilot array established in 2018 in the Subpolar NorthWest Atlantic (SNWA), a region of particular relevance in the marine carbon cycle. This area is a key region for anthropogenic carbon uptake and storage (Sabine et al., 2004; Gruber et al., 2009; Khatiwala et al., 2013; Racapé et al., 2018) as a consequence of (1) the Meridional Overturning Circulation (MOC) transporting warm and anthropogenic carbon-laden tropical waters by its upper limb (Sabine et al., 2004; Gruber et al., 2009; Khatiwala et al., 2013), and to (2) deep winter convection events occurring in the Labrador and Irminger Seas which transfer anthropogenic carbon from surface to the deep ocean (Körtzinger et al., 1999; Sabine et al., 2004; Ridge and McKinley, 2020). Moreover, it should be noted that the North Atlantic Oscillation (NAO), through its impact on the atmospheric variability in the North Atlantic region, induces high temporal variability on interannual (Watson et al., 2009) to decadal time scales (Leseurre et al., 2020) and may alter the residence time of anthropogenic carbon in the ocean by altering the rate of water mass transformation (Levine et al., 2011). In this context, the study region can be considered both a region of highest interest and a region of methodological challenges.

This paper illustrates the performance of the proposed standard Argo quality control routines with the float pH data acquired in the SNWA. By using float-pH data and independent pH data measured from water samples collected at nearby stations in the SNWA area, we can provide an evaluation of (1) the impact of the choice of the at-depth reference pressure as well as the choice of the reference method used to correct float-pH data, (2) differences to co-located in situ discrete pH data over the water column and within the surface layer and, (3) differences to crossovers to in situ surface pH data collected along a ship-of-opportunity line.

## 2 Materials and Methods

### 90 2.1 BGC-Argo float array

As part of an ongoing pilot study, 10 BGC-Argo floats from two manufacturers (NKE instrumentation and Teledyne Webb Research) were deployed in the SNWA region (Fig. 1) over the 2018–2022 period. All floats were equipped with pressure,



temperature, salinity (SBE-41CP sensor, Sea-Bird Electronics), oxygen (oxygen optode 4330 with individual multi-point manufacturer calibration, Aanderaa Data Instruments), and pH sensors (SeaFET<sup>TM</sup> sensor, Sea-Bird Electronics, Inc.). As some of  
95 BGC-Argo floats considered here are still operational, no DM data are available yet for the entire dataset. BGC-Argo data were  
obtained from the Coriolis Data Assembly Center. For inactive BGC-Argo floats, the Argo real-time quality control procedures  
have been applied by the Coriolis data centre (Wong et al., 2022). Temperature and salinity measurements (derived from con-  
ductivity) are recorded with accuracies of  $\pm 0.002$  °C and  $\pm 0.005$  PSU. The pH accuracy ranges from  $\pm 0.05$  as stated by  
the manufacturer to  $\pm 0.005$  after data is adjusted (Johnson et al., 2017) Oxygen optodes, similar to other chemical sensors,  
100 are known to suffer from storage drift prior to deployment (Bittig and Körtzinger, 2015; Johnson et al., 2015). SAGEO2, or  
an equivalent script, must therefore be used to correct float-oxygen data before any float-pH data correction which employs  
oxygen values as ancillary data (e.g., CANYON-B). We note that the oxygen data correction employs in-air measurements rou-  
tinely carried out during each float surfacing to achieve highest data accuracy (Bittig and Körtzinger, 2015; Bittig et al., 2018a).  
A stringent referencing and adjustment process for the oxygen can yield accuracies around  $1.5 \mu\text{mol kg}^{-1}$  (Bittig et al., 2018a).

105

In our case, O<sub>2</sub> from the 10 pH-equipped Argo floats was adjusted following Argo procedures and the adjustments are  
available in near-real time. In February 2023, one float had been recovered and five were still operational. We point out that,  
unfortunately, the 10 deployed floats suffered from an unusually high number of manufacturer-related technical issues or  
failures either of the pressure sensor (WMO 3901167, replaced from warranty by WMO 7900566), the GPS system (WMO  
110 7900566) or the pH sensor itself (WMO 6904110, 6904111, 6904112, 6904114, 6904115). This has severely compromised the  
amount of data acquired so far in the pilot study and reduces the robustness of the conclusions. As the two most long-lasting  
floats deployed in 2018 (WMO 3901668 and 3901669) showed stable pH data and the pH sensors have serial numbers not  
related to a recent problem with the pH sensor's reference electrode, they have been assumed to represent the optimum case for  
the achievable performance of this current technology. In addition, float-pH data measured by the float WMO 6904112 have  
115 been used in this study considering its position regarding the SOOP line transects and the high number of crossovers recorded.  
As a consequence, only float-pH data recorded by these three floats are used here. Moreover, adjusted temperature, salinity and  
oxygen data were available for these floats. We note, that the high failure rate points at problems in sensor manufacturing in  
recent years that need to be resolved in order for BGC-Argo to unfold its full potential.

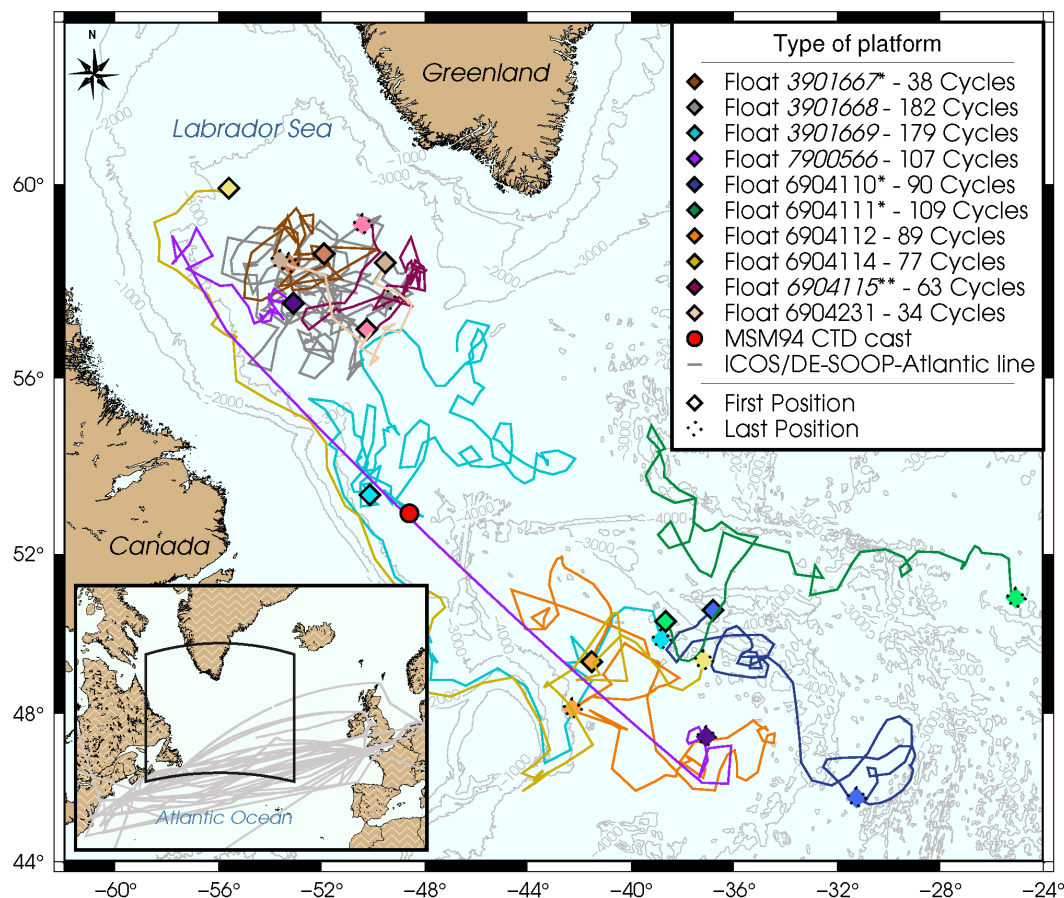


**Figure 1.** Map of the Northwest Atlantic with Labrador Sea and North Atlantic Current showing the trajectories of all 10 pH/O<sub>2</sub> floats deployed so far in our pilot study. In the legend, floats in italics are inactive. \* Float with a faulty pressure and/or pH sensor. \*\* Float recovered. Dotted points show the last locations as of February 7<sup>th</sup>, 2023. In the inserted map, gray lines indicate the ship routes occupied by our “Ship-of-Opportunity” platform (ICOS station DE-SOOP-Atlantic Sail). The red dot indicates the location of hydrographic station 13 visited during the *Maria S. Merian* cruise 94 (MSM94) in August 2020.

## 2.2 Reference measurements

120 In situ pH data measured from water samples other than the ones (e.g., GLODAP) used in the pH correction procedure are generally considered as reference data for float-based observations and are useful tools to independently estimate pH data accuracy and, if needed, apply additional corrections. Nevertheless, under normal circumstances, it would be nearly impossible to obtain specifically close crossovers between CTD casts and floats profiling during a float’s lifetime without significantly impacting the fieldwork schedule of a research cruise. The comparison of discrete samples for pH at a deployment cast with



125 float-pH data is limited due to the high sensor drift during the first cycles (Bittig and Körtzinger, 2015; Bittig et al., 2018a).  
Nevertheless, we had the unique opportunity to acquire a hydrocast with discrete pH samples with a float profile.

A few float (WMO 3901669) pH profiles occurred close to the R/V *Maria S. Merian* 94 (MSM94) cruise in August 2020 (Karstensen et al., 2020). Thanks to the cooperation of the chief scientist of the cruise and in a joint effort with the Euro-Argo RISE project, a spatio-temporally close crossover has been achieved: hydrographic station 13 with discrete sampling  
130 for pH analyses was achieved less than 1 day after and at the exact location of the float cycle 122 (Table 1, Fig. 1). The discrete samples were poisoned onboard following standard operating procedures (Dickson et al., 2007). They were measured at GEOMAR for total alkalinity (TA), dissolved inorganic carbon (DIC) and pH. Since DIC and pH are very sensitive to gas exchange they were measured in parallel as soon the bottles were opened. DIC was measured using a classical SOMMA system (Johnson et al., 1993) with coulometric detection, while pH was measured using the HydroFIA-pH system from 4H-  
135 Jena. The pH measurements were checked regularly against community-accepted certified reference material (CRM, Andrew Dickson, Scripps Institution of Oceanography, La Jolla/CA, USA). The resulting uncertainty in pH measurements for the discrete samples was  $\pm 0.002$  pH. The pH data were measured at 25°C and atmospheric pressure and were then converted to in situ temperature and pressure using the CO2SYS software (van Heuven et al., 2011). The matching of float-pH data and discrete pH data was performed in density space rather than depth space to avoid biases from internal wave activity.

140 In the SNWA, carbon observations are also carried out, among other programs, in the frame of the Ship Of Opportunity Program (SOOP; Goni et al., 2010). This program aims to obtain data from autonomous instrumentation installed on volunteer merchant ships regularly crossing the area. Parts of the Atlantic SOOP network are operated in the European Research Infrastructure ‘Integrated Carbon Observation System’ (ICOS) and the ‘Surface Ocean CO<sub>2</sub> Reference Observing Network’ (SOCONET). This network can be used as a potential reference for quality control of autonomous platform datasets as the  
145 standard-SOOP framework features, at least, routine  $p\text{CO}_2$  observations. GEOMAR has been operating, with intermissions, such a carbon-SOOP line for two decades in the Subpolar North Atlantic Ocean (ICOS station DE-SOOP-*Atlantic Sail*; Fig. 1). In addition to the standard  $p\text{CO}_2$  instrument (Model 8050  $p\text{CO}_2$  Measuring System, General Oceanics, Miami/FL, USA; Pierrot et al., 2009), autonomous systems for TA (Contros HydroFIA<sup>TM</sup> TA system, 4H-JENA engineering GmbH, Jena, Germany) and pH measurements (Contros HydroFIA<sup>TM</sup> pH system, 4H-JENA engineering GmbH, Jena, Germany) were installed  
150 on this SOOP line in 2019 and 2021, respectively. For pH, pre- and post-calibration runs against CRM from Andrew Dickson’s laboratory are performed before and after each 2.5 week roundtrip and an individual pH correction is applied to each pH indicator bag (meta-cresol purple; MCP). Note that the CRM is certified only for DIC and TA but pH measurements are also performed routinely for each bag and were made available to us (pers. comm. Andrew Dickson). The overall accuracy of SOOP-pH is estimated to be about 0.003 pH units.

### 155 2.3 Correction of float-pH data

Conceptually, the pH correction has to be done by adjusting the sensor’s reference potential ( $k_0$ ) as this is drifting over time (Johnson et al., 2016). For each pH sensor, the in situ pH is proportional to the voltage between the ion sensitive field effect transistor (ISFET) source and the reference electrode (Johnson et al., 2016). The measured potential is then converted into





**Table 1.** Crossover between pH prolines from the float WMO 3901669 and a CTD cast acquired in the Labrador Sea in August 2020. The time refers to end of profile.

Profile	Time	Position
Float WMO 3901669, Cycle 122	August 15 <sup>th</sup> , 2020 10:26 UTC	52.955°N-48.600°W
MSM94 CTD cast, Station 13	August 16 <sup>th</sup> , 2020 05:36 UTC	52.953°N-48.600°W

pH on the total proton scale using laboratory-based calibration coefficients. Thus, pH sensors are calibrated in the laboratory using spectrophotometric measurements and are therefore directly related to the laboratory calibration method. Each sensor's pressure and temperature coefficients, needed to compute the in situ pH, are also determined in the laboratory as described in Johnson et al. (2016). When deployed at sea, temperature changes modify the reference potential of the sensor and in return induce a sensor drift as the Nernst slope that transforms sensor potential to pH depends on temperature (Johnson et al., 2016, 2017).

The general adjustment process performed in the SAGE procedure is based on the assumption that the determined offsets and drifts are constant across the entire water column profile (Johnson et al., 2017). Thus, the standard SAGE adjustment process relies on a reference that is used to calculate the at-depth (typically around 1500 dbar) anomaly between measured and estimated reference data, which is applied as an offset to the reference potential. It is propagated on the entire water column profile by normalizing the adjustment along the profile to the temperature at which the adjustment was derived. Temperature-normalized changes in pH are calculated by multiplying the change in pH computed at depth by the ratio of the absolute temperature of the sample to the absolute temperature at reference depth. To calculate the correction, the float-pH time-series is split into distinct segments bound on either side by breakpoint nodes determined by a cost function. Then, both drift and offset between segments are calculated by linear least-squares fit to the anomaly data series between two nodes.

In our analysis, a pH correction method called "linear adjustment" has been implemented locally. Like in the SAGE tool, the pH correction is calculated by this method based on the comparison to reference CANYON-B pH values calculated at a user-defined pressure level, where spatiotemporal variability of oceanic components is assumed to be minimal. The CANYON-B method was chosen as a reference assuming it to be more robust in the North Atlantic region (Carter et al., 2021). Nonetheless, two slight differences exist between SAGE and the method proposed here: (1) The correction can be applied either to each cycle or, as in SAGE, to data within segments of consecutive profiles (with each segment calculated using a cost function). (2) When using the segment method, a centered 7-point linear regression is used for cycles neighboring segment breakpoints to allow for a smoother  $k_0$  drift between segments (Fig. 2; Johnson et al., 2016). As in SAGE, offset and drift calculated with this method are then applied to the measured float pH profiles after normalization to the temperature at which the adjustment was derived. Finally, another correction method entitled "3-point running mean" was tested in this study. In this, the correction calculated for each cycle (cycle-by-cycle method) was used to determine a new offset for each cycle calculated using the mean value

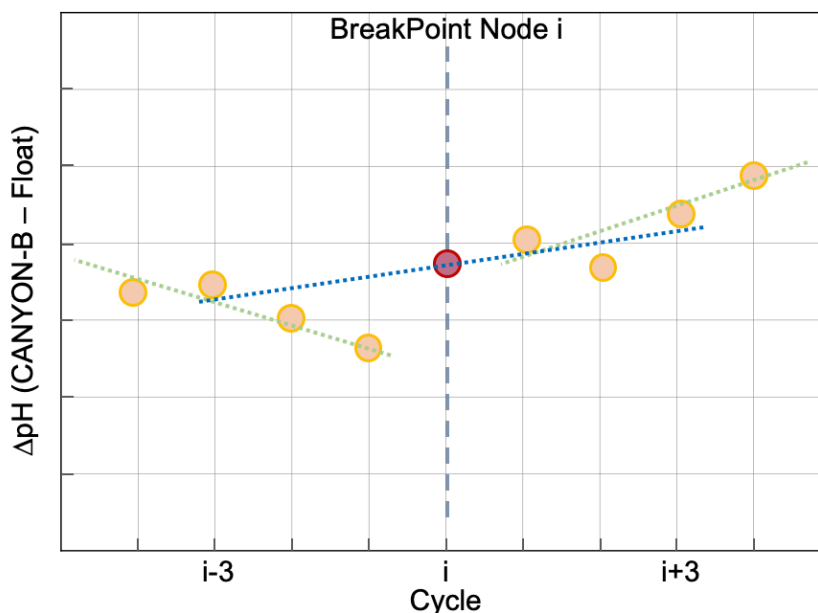


**Figure 2.** Schematic representation of the GEOMAR float-pH data correction method. As in the SAGE tool, a linear least-square fit is calculated between reference and float-pH data for cycles located between two breakpoint nodes to derive the offset and drift (green lines). The blue line represents the second least-square fit obtained and applied to the elements located 3 cycles before and after the node (red dot) in the GEOMAR method. Adapted from Maurer et al. (2021).

185 for the offset of the cycle before and after the considered one. This method should smooth the correction obtained with the cycle-by-cycle adjustment. Hereafter, every correction method different from the one in SAGE will be labelled as GEOMAR method.

## 2.4 Comparisons with SOOP-based observations

To compare SOOP-based and float-based surface pH observations, we adopted the crossover definition from the Surface  
190 Ocean CO<sub>2</sub> Atlas (SOCAT; Sabine et al., 2013) which combines the mismatch in both distance and time between two measurements. In the SOCAT algorithm, one day of separation in time ( $t$  in days) is heuristically equivalent to 30 km of separation in space ( $x$  in km) and 80 km is the maximum value for an acceptable crossover  $((dx^2 + (dt*30)^2)^{1/2}$ ; Wanninkhof et al., 2013). Here we used an increased search window of 400 km to yield a larger number of crossovers and to optimize between spatial and temporal mismatch. In addition, a maximum temporal mismatch of 7 days was allowed for a crossover. The SOCAT criterion  
195 of a maximum of 80 km aims to compare two data sets of surface  $p\text{CO}_2$  observations to agree better than  $2 \mu\text{atm}$ . In this study, we conclude that this is yet not satisfied by pH data from floats and therefore we used a larger radius to ensure more crossovers and better statistics. The resulting crossovers were further reduced by the requirement of a maximal temperature difference between the float measurement and the temperature measurement onboard the SOOP line of  $4^\circ\text{C}$  ( $-4.0 < \Delta T < 4.0$ ). To make the





pH measurements from both platforms comparable, the SOOP-based pH data were corrected to the surface water temperature  
200 of the corresponding float profile. We note that for possible future implementation of the SOOP crossover method in the DM  
QC routine for float pH data this needs to be further explored and more elaborate crossover criteria need to be developed.

## 2.5 MLD calculations

Following De Boyer Montégut et al. (2004), a density threshold of  $0.03 \text{ kg m}^{-3}$  with a reference depth of 10 dbar was  
used to compute the Mixed Layer Depth (MLD). We used MLD to determine waters affected by deep convection events which  
205 cause unstable biogeochemical properties also at depth that are being used for float-pH data.

## 3 Results and Discussion

### 3.1 Uncertainties of delayed-mode float-pH data

In the following we first illustrate uncertainties associated with the current correction method for float-pH data as imple-  
mented in the standardized routines from Argo data management as well as in the SAGE tool for two referencing methods  
210 (CANYON-B and LIRPH) and two selected floats (WMO 3901668 and 3901669) which had no technical malfunctions during  
their lifetime.

#### 3.1.1 Uncertainty associated with choice of reference depth

In order to assess the uncertainty associated with the choice of the reference depth for pH correction, differences between  
float-pH data corrected using the “classical” reference pressure around 1500 dbar (Maurer et al., 2021) minus float-pH data  
215 corrected over the pressure range 1940 and 1980 dbar were calculated for the two reference methods LIRPH and CANYON-B  
(Fig. 3A). Calculated differences between float-based pH data processed using corrections based on the two different depth-  
reference pressure values ranged between  $-0.0003$  and ca.  $0.02$  pH units, with mean values for all cycles of the considered floats  
varying between  $0.0068$  and  $0.0098$  pH units (Fig. 3A). The choice of the reference depth thus incurs a large difference of ca.  
 $0.01$  pH units which is above a tolerable level. In this deep convection area, it therefore points to a severe limitation of the pH  
220 correction scheme. The deepest mixed layer depth estimated from the float time-series was at 1937 dbar which, showing that  
the entire water column covered by the float profiles is probably affected. In this regard, the subpolar North Atlantic region  
with its deep-reaching anthropogenic  $\text{CO}_2$  imprint is a difficult area for the unambiguous choice of a stable and unperturbed  
reference depth. Recently, Fiedler et al. (2022) performed a similar exercise by changing the reference depth from ca. 1500  
dbar to 1000 dbar for a float in the Eastern Tropical North Atlantic region and reported a tolerable uncertainty from this choice  
225 of  $0.0008$  pH units. The order of magnitude difference in the uncertainty incurred from the reference depth choice illustrates  
the regional dependence on hydrological conditions which can severely compromise the correction method or even render it  
almost useless as in the case presented here.

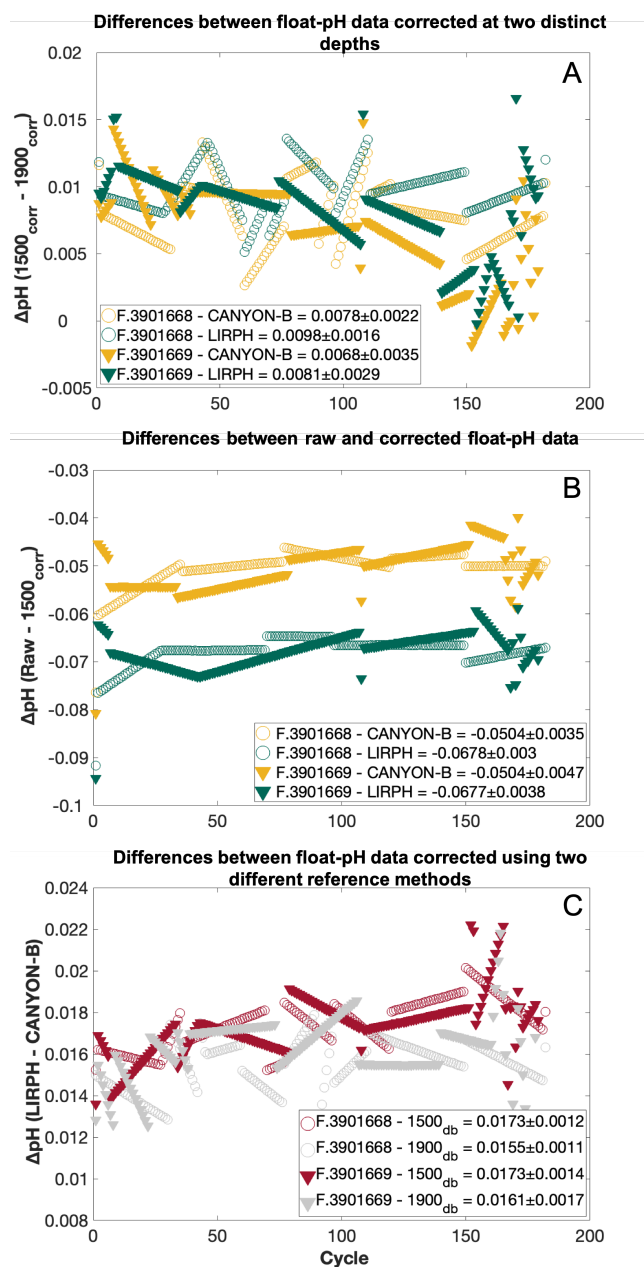


**Figure 3.** (A) Mean differences between float-pH data corrected using the “classical” reference depth of 1500 dbar minus float-pH data corrected with reference-pH data calculated between 1940 and 1980 dbar for the floats WMO 3901668 (circle dots) and 3901669 (triangle dots) and for the two reference methods LIRPH (green dots) and CANYON-B (orange dots). (B) Raw float-pH data minus float-pH corrected using the “classical” reference depth of 1500 dbar for the two-reference methods CANYON-B (orange dots) and LIRPH (green dots) and for the floats WMO 3901668 (circle dots) and 3901669 (triangle dots). (C) Float-pH corrected using LIRPH as a reference method minus float-pH corrected using CANYON-B as a reference method according to two distinct reference pressure depths (1500 dbar depth - red dots, 1900 dbar - gray dots) for the floats WMO 3901668 (circle dots) and 3901669 (triangle dots).



### 3.1.2 Uncertainty associated with choice of reference model

230 Two distinct reference methods are used in the standardized Argo pH quality control, both in SAGE and in this study: the LIR pH regression method (LIRPH) and the CANYON-B method (Fig. 4). For both methods, uncorrected float-pH showed a significant offset to the reference pH profiles (Fig. 3B). Moreover, a mean difference between the two reference methods of about 0.016 pH units is observed in the SNWA (Fig. 3C).

235 While the CANYON-B and the LIRPH algorithmic methods are methodologically different (one is based on a neural network while the other uses linear regressions), both have been trained with the GLODAPv2 data set (Olsen et al., 2016) and tested against it. Still, ocean pH measurement practices have changed with time, leading to a variety of ways to measure. In addition, pH calculated from DIC and TA is not always in line with spectrophotometrically measured pH (Carter et al., 2018). In consequence, heterogeneities in pH data compilations such as GLODAPv2 exist. While CANYON-B was trained with GLODAPv2 without modifications, Carter et al. (2018) applied a range of corrections to create a more consistent pH  
240 data product that was used for LIRPH training (with pH being in line with “purified spectrophotometric pH measurements”). Given the dominance of calculated pH data in GLODAPv2, CANYON-B pH estimates are in line with calculated pH (Bittig et al., 2018b; Carter et al., 2018). In the SAGE software, an optional CANYON-B pH data adjustment can be applied to align estimates with spectrophotometric pH measurements made using purified dye following Carter et al. (2018, Equation 1). The recent literature (Carter et al., 2018; Johnson et al., 2018) recommends employing this reference-pH data adjustment  
245 emphasizing that, as pH sensors are calibrated in the laboratory using spectrophotometric measurements with purified dyes, sensor measurements should be directly related to the laboratory calibration method. In this study, we have decided to keep this reference-pH data adjustment to correct float-pH data.

Therefore, it is more critical than ever for the scientific community to perform intercomparisons of marine CO<sub>2</sub> system variables and address their associated uncertainties regarding the large and growing variety of instruments and approaches  
250 used to measure, deduce and calculate CO<sub>2</sub> variables (Fig. 4). Despite the undeniable strength of current algorithms, they both suffer from weaknesses and uncertainties due to the pH adjustment, limiting the one (LIRPH) from a complete regional or temporal description of the current ocean acidification (Carter et al., 2018) and the other (CANYON-B) from a conversion of the pH according to another measurement mode (Bittig et al., 2018b). In consequence, a mean difference between the two methods of about 0.016 pH units is observed in the SNWA (Fig. 3C). In addition, using the SOCCOM array, Maurer et al.  
255 (2021) calculated CANYON-B and LIRPH pH estimates and observed a larger uncertainty toward the surface compared to 1500 m with mean differences (CANYON-B pH minus LIRPH pH data) of -0.025 and 0.001 pH units, respectively. This surface discrepancy can be explained by the difficulty for algorithms to represent seasonal variability and air-sea gas exchange.

Thus, this study illustrates the need for further studies on the choice and performance of the referencing method in different ocean regions with a special emphasis on regional biases and limitations.

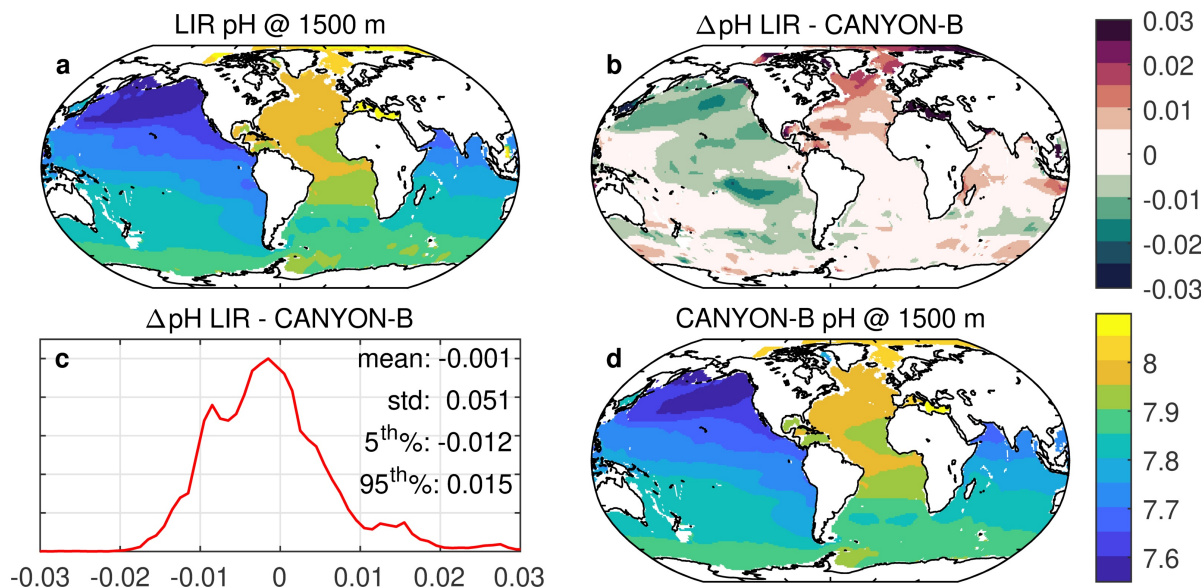


**Figure 4.** Spatial distributions of estimated pH data at 1500 m using different reference models: LIRPH (A) and CANYON-B (D). The map of the spatial difference between the two estimated pH datasets is presented in panel (B). Panel (C) shows the bias  $\Delta\text{pH}$  distribution (with statistics). The upper colorbar indicates the difference between estimated pH data using the two models and the lower colorbar gives the pH values.

### 260 3.1.3 Correction of sensor drift

In addition to the choice of reference depth and method, some additional uncertainty can be incurred by the way how the pH sensor drift correction is applied to the float data. Sensor response often shows different modes of variability and drift. A typical mode of variability is sensor noise, i.e. variability entirely introduced by electronic components of the sensor. This noise does not represent true variability in the observed quantity and should therefore be removed. In addition, long-term systematic drift in sensor response due to changes in zero levels and/or gain factors is also an internal artefact of the sensor that needs to be corrected for. More rarely, sensors can also show more erratic and non-systematic variability in individual measurements or over certain measurement periods which often has unknown reasons. These are hard to distinguish from true variability in the observed quantity and are hence also hard to correct for. The method to apply sensor corrections in time-series measurements should take a conservative approach trying to remove known modes of sensor variability while conserving real variability in the data.

The sequence of steps in the current Argo correction method uses is a delayed mode correction and first the  $\Delta\text{pH}$  (raw-corrected, at reference depth) is calculated for each cycle. In the SAGE tool, a cost function is applied for the correction of temporal trends that determines sections over which a linear correction is calculated and then applied to each cycle included in the respective section (Fig. 5). We also applied three different correction methods: (1) a cycle-by-cycle correction, (2) a 7-point



275 linear regression method named “linear adjustment” and (3) a 3-point running mean correction method, which should smooth the correction obtained with the cycle-by-cycle adjustment. In every case, CANYON-B was used as the reference method as well as the “classical” reference pressure depth of 1500 dbar.

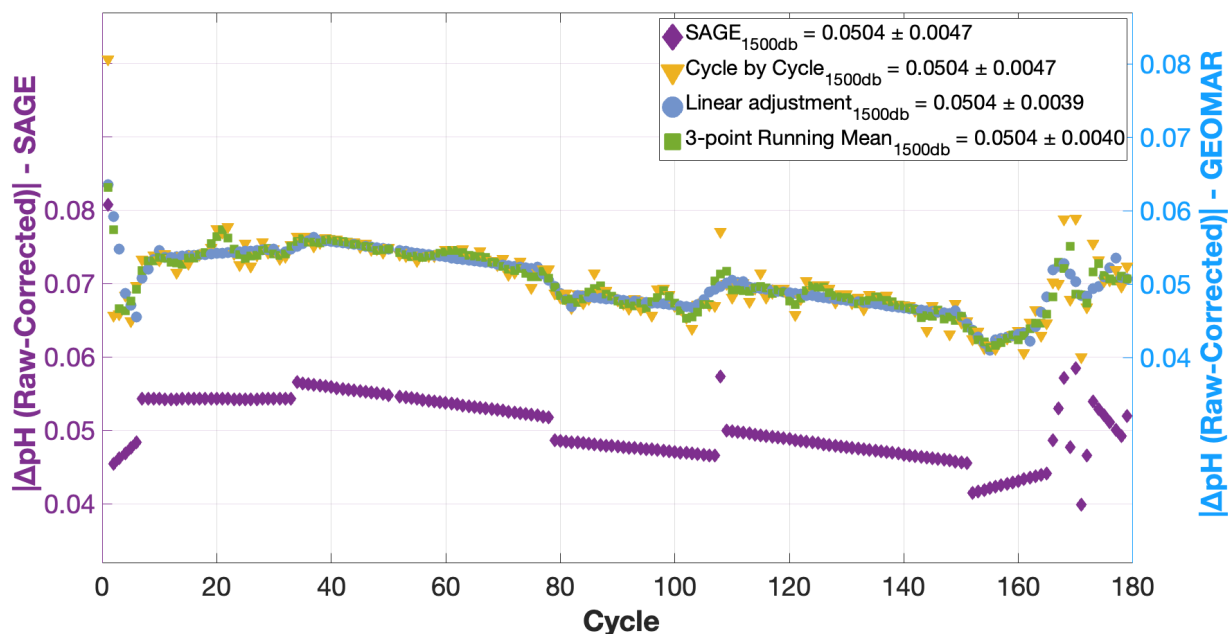


**Figure 5.** Differences between raw float-pH data minus float-pH corrected using the SAGE tool (purple dots, left y-axis), the cycle-by-cycle GEOMAR method (yellow dots, right y-axis), and the linear mean regression GEOMAR method (blue dots, right y-axis) for float WMO 3901669. The 3-point centered running mean correction method is represented by the green dots (right y-axis). In every case, CANYON-B was chosen as a reference method and 1500 dbar were chosen as reference depth. Note that we put the data obtained with the SAGE tool and those calculated using the GEOMAR correction on two separate y-axes for better viewing.

The profile-by-profile correction has the disadvantage that it does not remove any of the sensor noise. On the other hand, a single linear drift correction across the entire time-series does not seem adequate either as it does not reflect the clear upward and downwards swings in the record which are mostly interpreted as changes occurring in the sensor. Therefore, a more adapted method, which includes a higher order spline fit, a centered running mean or segment separation of the record into linear drift phases has to be applied. The latter is implemented in the SAGE tool (Fig. 5). This method, however, does not provide smooth transitions between linear drift phases and leads to step-like changes of the order of 0.01 pH units between two consecutive profiles which appear to be unrealistic when compared to the pattern of the profile-by-profile correction. The correction methods for temperature and salinity also ask for maximum smoothness in the corrections and to avoid introducing artificial jumps (Owens and Wong, 2009). Our slightly improved GEOMAR linear adjustment version (Fig. 5 top) significantly reduces these discontinuities and artificial jumps. Generally, the linear segment methods assume linear sensor drift and step-like changes in sensor characteristics. In our view, the sensor rather shows undulations in response with smooth and less smooth



phases. The pH sensor behavior when the float drifts at its parking depth is in agreement with this observation (Fig. A1). Such  
290 a pattern can perhaps be best corrected for with our modified GEOMAR segment method or alternatively with a spline fit or a  
3-point centered running mean (Fig. 5 top).

We suggest to use the improved segment or running method to avoid strong discontinuities in the pH correction which  
otherwise could introduce biases in corrected pH of up to 0.01 pH units in individual profiles – a magnitude that would  
strongly impair quality control measures based on referencing against other in situ pH measurement from CTD casts or surface  
295 observation platforms (see Section 3.2).

## 3.2 Comparison with in situ discrete pH

### 3.2.1 Crossover with CTD hydrocast

Crossover comparisons can be used as an option to independently estimate float-pH data accuracy and determine if addi-  
tional corrections are needed. In 2020, we had the rare opportunity to perform a CTD hydrocast with discrete pH sampling  
300 (cruise MSM94) at the exact location and less than 24 h after a float profile (WMO 3901669, profile 122; Fig. 1) which allows  
for direct comparison between discrete and float-based in situ pH data after the float's initial drift period (Fig. 6C). We find  
mean differences of -0.0485 and -0.0424 pH units (Fig. 6C) between the reference pH cast and the fully corrected pH of cycle  
122, with the higher difference found for the “classical” reference depth of 1500 dbar.

Matching sensor data from a float with discrete samples is a non-trivial task due to complications arising from (a) the sensor  
305 response time and (b) the uncertainty about the effective depth from which the water captured in a Niskin bottle at a trigger  
given depth stems from. There seems to be no perfect way of matching these and some uncertainty remains – especially in-  
depth ranges with strong gradients in the variable of interest. Mismatch (and resulting statistical noise) due to internal wave  
activity can mostly be avoided by matching profile and bottle data in density space which was performed here. However, the  
likely imperfect representation of the true water sampling depth by the trigger depth (and hence corresponding CTD data) of  
310 a Niskin bottle introduces the potential of systematic error in gradient regimes, although in a gradient of increasing pH both  
effects (a) and (b) would lead to underestimation of pH. Still, the results of this comparison therefore have to be interpreted  
with caution.

The results show smallest offsets at/near the reference pressure levels and increase towards the surface. In this area, near-  
surface variability and patchiness can be large and would require a perfect match in both space and time for strong conclusions  
315 and robust significance of the surface values observations (< 30 dbar). Nevertheless, pH offsets are positively correlated with  
temperature, being smallest at the temperature of the reference depth. Overall, the results appear to be robust and not an artefact  
of the matching procedure and point towards an imperfect representation of the temperature and pressure dependences of the  
pH sensor (Fig. 6D). Although the actual pH values may be slightly different due to the regional variability, the observed  
trend is confirmed. However, this single crossover does not allow for a solid conclusion and therefore can only serve as a  
320 hint at shortcomings in the pH referencing method. With larger amounts of matchups between hydrocasts and pH profiles and



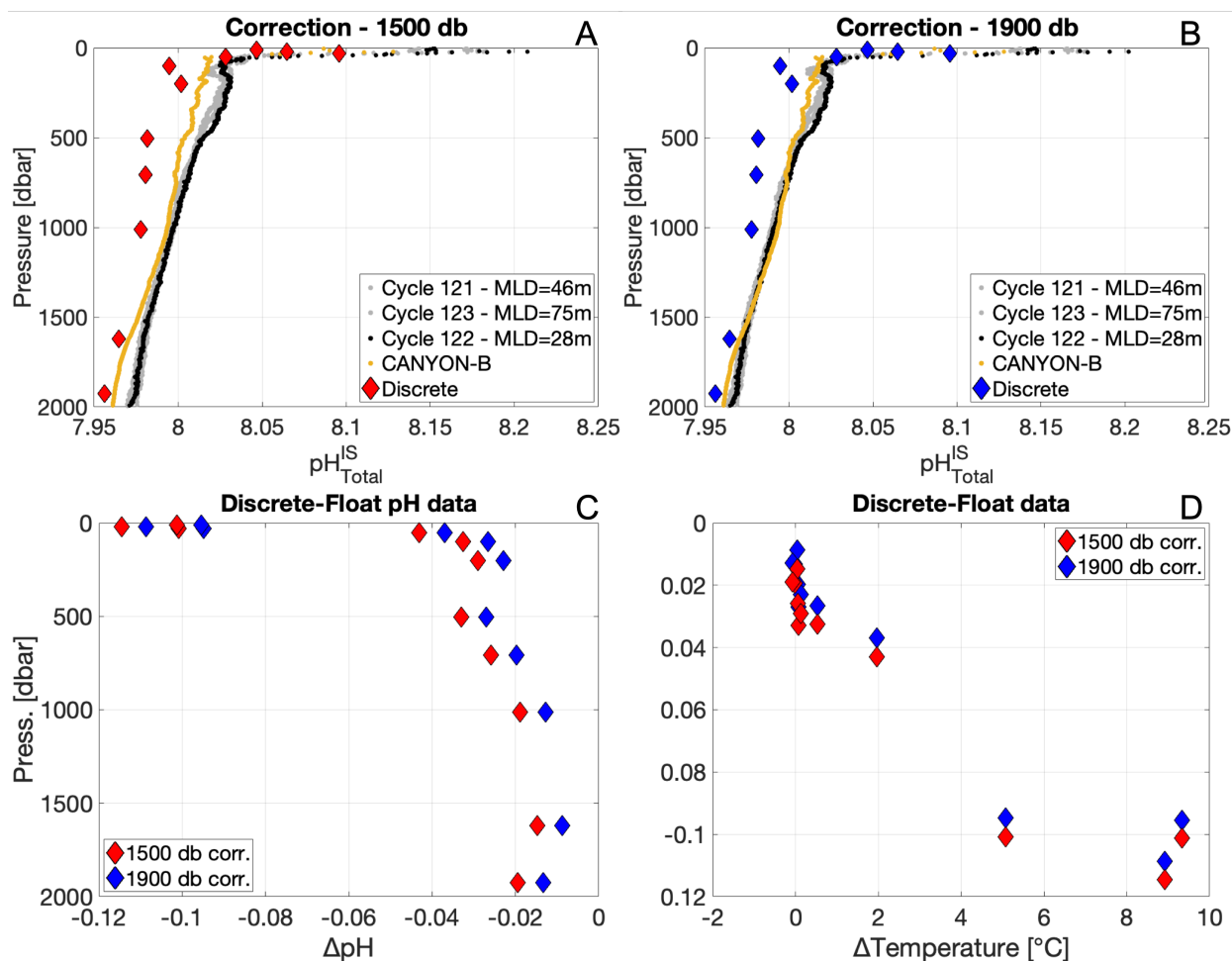


**Figure 6.** (A and B) Vertical profiles of pH in total scale at in situ temperature measured during the MSM94 cruise and acquired by the float WMO 3901669 during cycles 121, 122 and 123 (gray and orange lines, respectively). Float-pH data have been corrected using the SAGE tool with CANYON-B (black lines) as reference method using reference levels of 1500 dbar (A) and 1900 dbar (B). (C) Differences between discrete and float-pH data (for the cycle 122) calculated after matching in density space to avoid biases from internal waves. The color code refers to float-pH data corrected using reference levels of 1500 dbar (red diamonds) and 1900 dbar (blue diamonds). (D)  $\Delta$ pH as a function of the difference between discrete water temperature and temperature values recorded at the depth where float-pH data have been calculated to obtain the  $\Delta$ pH.

optimized SOOP-float crossover data, an independent validation and perhaps correction method could be investigated. Indeed, SOOP data can represent an additional reference and comparison data source.



### 3.2.2 Crossover with SOOP-based surface measurements

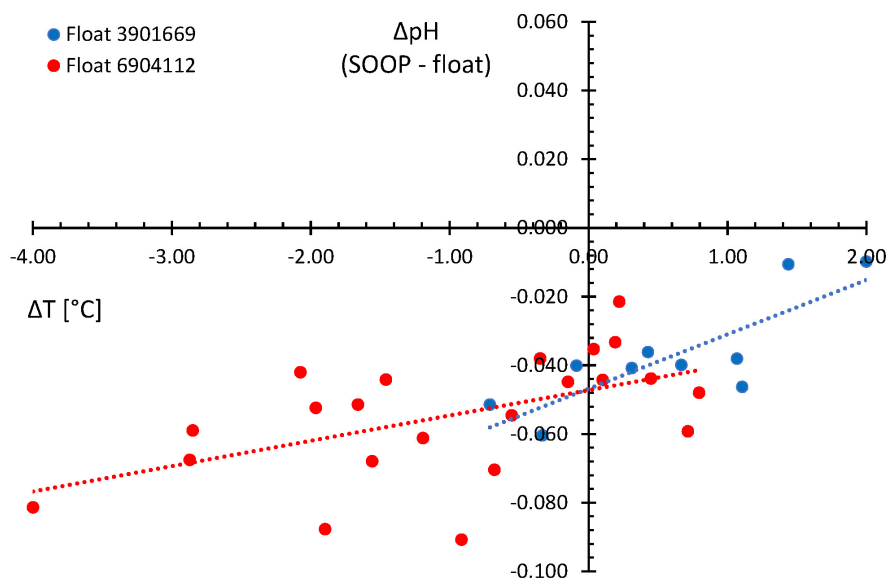
In addition to the comparison of whole pH profiles as described above, we compared float-based pH measurements in the surface (average pH between 5 and 15 m depth) with surface pH measurements from a SOOP line crossing the North Atlantic every 5 weeks (see Section 2.4). The cruise track of the SOOP line crosses the area of the floats deployed in the North Atlantic Drift region (see Figure 1). For this comparison, we used data from two floats (WMO 6904112 and WMO 3901669) between May 2021 and October 2022. We note that further testing and improvement of this approach on larger datasets need to be carried out to define an optimal crossover criterion. Given the limitations of the dataset (mostly due to massive manufacturing problems of the 2020/2021 pH sensor series), no robust recommendations can be drawn from these experiments. Nevertheless, the assumption was made hereafter that regressions using crossovers achieved with a relatively wide search window yield a more robust  $\Delta\text{pH}$  estimate as an average of a small number of crossovers found with a smaller search window.

Figure 7 shows the differences ( $\Delta\text{pH} = \text{SOOP} - \text{float}$ ) between SOOP-based surface pH observations and the averaged mixed layer pH values of the two pH/O<sub>2</sub> floats as a function of  $\Delta T$ . Under the assumption that differences in pH to a major extent are driven by differences in temperature, the  $\Delta\text{pH}$  at  $\Delta T = 0$  should be a reasonable estimate of the pH offset between SOOP and float. By fitting a linear regression to the data, the pH offset at  $\Delta T = 0$  can be estimated more robustly. We want to point out that this analysis has its limitations: (1) the study area is characterized by high surface variability due to mixing, (2) the presented analysis uses only data from 2 floats during an 18-month period. However, the comparison between float-based pH and SOOP-based pH indicates that surface pH is very consistently biased high by 0.047 pH units for the two floats. This apparent bias is in the same direction (albeit a factor of 2 smaller) than what was found in the comparison with discrete CTD cast samples for surface waters. This suggests a systematic problem with float-based pH in the surface.

Table 2 summarizes the statistics associated with these crossover analyses. Standard deviations of the averages give an indication of the coherence of the extracted dataset and hence their statistical weight. The average  $\Delta T$  of the crossovers is within  $\pm 1^\circ\text{C}$  for each float (Table 2) with the corresponding  $\Delta S$  on the order  $\pm 0.5$ . This indicates that the water mass correction achieved through the regression approach is reasonably effective. Also, calculating the pH offset as a function of  $\Delta S$  (data not shown) yields  $\Delta\text{pH}$  values which are statistically indistinguishable from the ones based on  $\Delta T$ . In conclusion, despite the limited number of floats and crossovers associated with this study, the preliminary results point at unacceptably high and almost identical biases in surface pH values from the 2 floats (as seen by the values crossing the y-axis), which have been corrected in the exact same way. This highlights that the present instructions to correct pH by a unique offset established at-depth are insufficient, at least in our study area. An improved understanding of the temperature (and pressure) effect on the (individual) sensor as well as a systematic correction with carbon measurements could be the way forward to improve float-pH data adjustment.

### 3.3 Implications and changes in ocean chemistry

In the following, we illustrate the implications of the identified uncertainties in the current DM process for float-pH data on the calculation of other parameters of the marine CO<sub>2</sub> system, and the resulting limitations for data products and scientific appli-



**Figure 7.** Offsets between SOOP pH and fully corrected float pH (y-axis) as a function of temperature difference (x-axis) for crossovers ( $\Delta x \leq 400$  km,  $\Delta t \leq 7$  d,  $\Delta T \leq 4^\circ\text{C}$ ) of three different floats. Float-pH data have been corrected with the SAGE tool using the classical reference depth (around 1500 dbar) and CANYON-B as reference.

**Table 2.** Statistics of the crossover analysis for SOOP- and float-pH data. SD stands for Standard Deviation.

Float WMO	$\Delta\text{pH at } \Delta T=0$		$\Delta T$		$\Delta S$	
	Mean	SD	Mean	SD	Mean	SD
3901669	-0.047	0.004	0.87	1.00	0.41	0.50
6904112	-0.047	0.004	-0.98	1.29	-0.40	0.58

cations. BGC-Argo float-based pH data can potentially be a very powerful tool to estimate the ocean  $\text{CO}_2$  sink when converted to  $p\text{CO}_2$  in combination with a second marine  $\text{CO}_2$  system variable such as DIC or TA. While float-based observations for both DIC and TA are still lacking, and as TA values are readily predictable thanks to many algorithms (e.g., the Locally Interpolated Alkalinity Regression (LIAR) method; Carter et al., 2018) and also less impacted by biological variations (Zeebe and Wolf-Gladrow, 2001), TA is the parameter of choice to derive  $p\text{CO}_2$  values. Current understanding (e.g., Carter et al., 2018) is that TA can be predicted with a typical uncertainty of about  $6 \mu\text{mol kg}^{-1}$  which does not include, however, potential regional biases due to insufficient data coverage as well as biases due to unknown organic TA contributions in highly productive and/or



coastal waters. Using this TA uncertainty,  $u(\text{TA})$ , we calculated the minimum required pH uncertainty,  $u(\text{pH})$ , that allows to meet two  $p\text{CO}_2$  uncertainties,  $u(p\text{CO}_2)$ , as defined by Newton et al. (2015): the “climate goal” uncertainty of  $2 \mu\text{atm}$  and the “weather goal” uncertainty of  $10 \mu\text{atm}$  (Fig. 8).

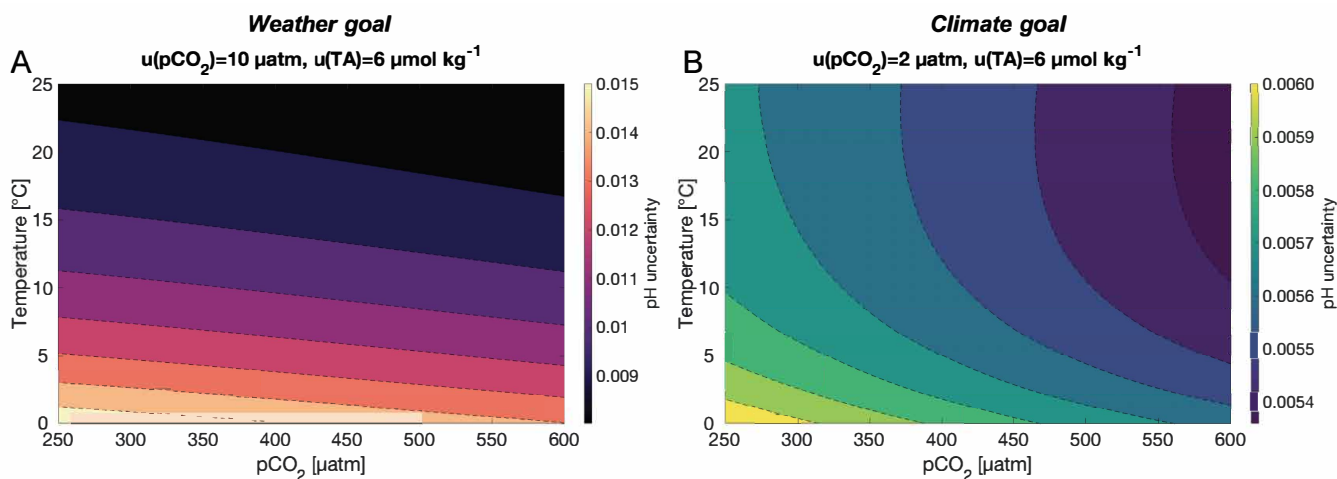


**Figure 8.** Uncertainties in pH allowed to derive  $p\text{CO}_2$  data as a function of temperature and  $p\text{CO}_2$ , using uncertainties of  $10 \mu\text{atm}$  (A) and  $2 \mu\text{atm}$  (B) for  $p\text{CO}_2$  and an uncertainty in TA of  $6 \mu\text{mol kg}^{-1}$ .

As shown in the Figure 8A,  $p\text{CO}_2$  can be calculated with an uncertainty of  $10 \mu\text{atm}$  when using pH uncertainties of around 0.01 pH units (from 0.008 to 0.016 depending on T and  $p\text{CO}_2$ ), and thus reach the “weather goal” (Newton et al., 2015) which defines maximum uncertainties of  $\pm 10 \mu\text{mol kg}^{-1}$  for TA/DIC, of  $\pm 0.02$  pH units and  $\pm 2.5\%$  for the  $p\text{CO}_2$  (ca.  $10 \mu\text{atm}$  at  $400 \mu\text{atm}$ ). To derive  $p\text{CO}_2$  data with an uncertainty as the one defined by the “climate goal” criterion, and considering a  $u(\text{AT})$  equals to  $\pm 6 \mu\text{mol kg}^{-1}$ , a pH uncertainty  $< 0.006$  pH units is required (Fig. 8B).

At  $u(\text{TA}) = 6 \mu\text{mol kg}^{-1}$ , the overall contribution of this parameter to the derived uncertainty in  $p\text{CO}_2$  is rather marginal in comparison to the dominant impact of  $u(\text{pH})$ , and the resulting  $p\text{CO}_2$  change represents slightly more than 16% of the pH impact when considering a 0.006 pH units pH-uncertainty. In other words, the uncertainty in predicted TA corresponds to an uncertainty in pH of about 0.001 pH units. In consequence, and while the  $u(\text{TA})$  is not the major obstacle to derive accurate  $p\text{CO}_2$  data, estimated TA value still would have to be carefully estimated to then be used as a predictor variable. Regional and/or seasonal biases in estimated TA can be observed in some oceanic regions where high nutrient concentrations can occur, especially during phytoplankton bloom situations. The TA-uncertainty can also be more important in areas subject to terrestrial discharges as allochthonous matter or organic TA can be associated with non-carbonate alkalinity (Soetaert et al., 2007; Hunt et al., 2011). This perhaps warrants specific tests on the accuracy of TA predictions in critical regions (or seasons).

In order for float-pH data to be suitable for the calculation of parameters of the marine  $\text{CO}_2$  system, and in particular  $p\text{CO}_2$  data, with useful accuracies, the documented shortcomings in accuracy of float-pH need to be explored and addressed. Taking into account the error propagation, the  $u(\text{pH})$  allowed for calculating  $p\text{CO}_2$  from the pH and TA is on the order of  $0.0107 \pm$



0.0018 for the weather goal and  $0.0056 \pm 1.42 \times 10^{-4}$  for the climate goal. In the SNWA region, this study has shown that the combination of uncertainties associated with the choice of the reference method and reference depth as well the choice of method to calculate the corrections for the individual float cycles can lead to uncertainties in pH well beyond what is deemed acceptable to exploit the pH data for CO<sub>2</sub> calculation purposes. Our findings indicate that large biases in float-pH can occur, particularly in the surface ocean where the data are likely of the highest scientific interest and relevance. Thus, to achieve the required *p*CO<sub>2</sub> uncertainty, it is desirable to reduce and better constrain the uncertainty associated with float-based pH measurements to derive and depict entirely the oceanic carbon cycle.

#### 390 4 Conclusions

For correcting float-based pH measurements, the current standardized routines from Ago data management rely on a single-point at-depth correction method along with reference algorithms such as LIRPH or CANYON-B, assuming that the adjustment calculated at-depth yields corrections applicable to the entire profile

By using both, float-based pH data and in situ pH data from other platforms acquired in the SNWA area, this study was able to identify uncertainties and shortcomings associated with the correction applied which raise concerns about the single at-depth correction on adjusted pH data. Our findings show consistent results indicating that corrected float-pH data may be biased by several hundredths of a pH unit near the surface in the SNWA in response to deep convection events, suggesting that similar observations might be possible in other deep convection regions. Even if the statistical significance of our findings is limited due to the low number of comparisons available, this apparent weakness of the DM QC process of float-pH data should be considered in light of the challenges in interpreting TA and pH-derived *p*CO<sub>2</sub> data in a crucial area for ocean convections events and anthropogenic carbon storage. With regards to the situation observed in the SNWA, we suggest (1) to revisit the temperature and pressure effect on the sensor, (2) to better assess the impact of biological processes on the pH estimate and (3) to consider global crossover analysis between float-pH surface data and other platforms (SOOP lines, buoy, floats) to independently quality controlled and perhaps correct float pH data close the surface, where the accuracy required to better constrain the oceanic response to climate changes is the highest.



*Data availability.* Data from the German-SOOP *Atlantic Sail* line are available at [https://meta.icos-cp.eu/resources/stations/OS\\_NA-VOS](https://meta.icos-cp.eu/resources/stations/OS_NA-VOS). Argo data are available at <http://doi.org/10.17882/42182#96550> or at <ftp://ftp.ifremer.fr/ifremer/argo/dac/coriolis>. These data were collected and made freely available by the International Argo Program and the national programs that contribute to it (<https://argo.ucsd.edu>, <https://www.ocean-ops.org>). The Argo Program is part of the Global Ocean Observing System. Data from the MSM94 cruise ([https://doi.org/10.48433/cr\\_msm94](https://doi.org/10.48433/cr_msm94)) can be found on the Pangea website (<https://doi.pangaea.de/10.1594/PANGAEA.927311>).

*Author contributions.* CW-R, TS, and AK initiated and designed the study. TS, and AK helped supervising the study. BK and HB helped revising the manuscript and providing significant inputs. CW-R, TS, and A.K. wrote the first draft of the manuscript. All the authors contributed to manuscript revision, read and approved the submitted version.

*Competing interests.* The authors declare that they have no known competing financial interests or personal relationships that could have appeared to influence the work reported in this paper.

*Acknowledgements.* This work has received funding from the European Union's Horizon 2020 Research and Innovation Program in the Euro-Argo RISE project (grant agreement n°824131). It was further supported by the projects DArgo2025 (FKZ 03F0857A+C) and C-SCOPE (FKZ 03F0877A+B) of the German Ministry for Research and Education. We would like to thank Johannes Karstensen, chief scientist of cruise MSM 94, and his team for wonderful cooperation in the context of the achieving a crossover with one of our floats.





## 420 Appendix A: Supplementary Material

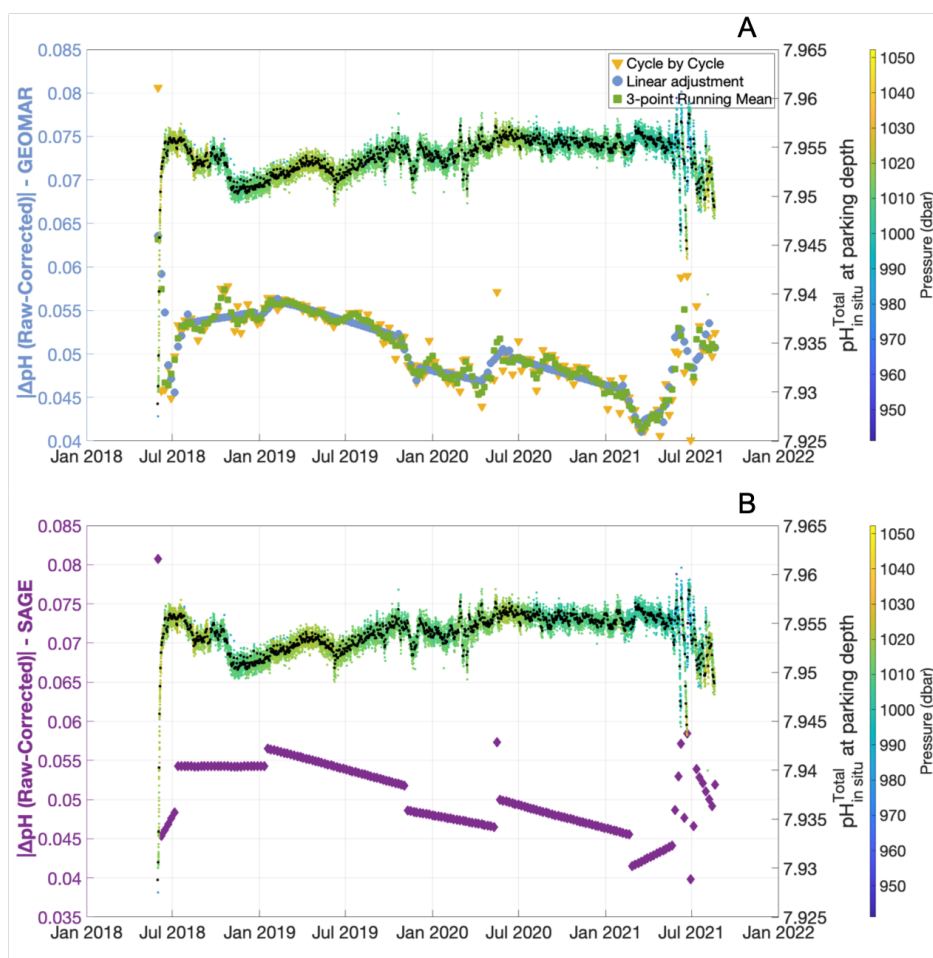


**Figure A1.** (A) Differences between raw float-pH data minus float-pH corrected using the cycle-by-cycle GEOMAR method (yellow dots, left y-axis), the linear mean regression GEOMAR method (blue dots, left y-axis) and the 3-point centered running mean correction method (green dots, left y-axis). (B) Differences between raw float-pH data minus float-pH corrected using the SAGE tool (purple dots, left y-axis). On every plot, the pH measured at the parking depth (right y-axis) has been added and the colorbar indicates the pressure. Black dots represent mean pH values for each day. For the correction, in every case, CANYON-B and 1500 dbar were chosen as reference method and reference depth, respectively.



## References

- Abram, N., Gattuso, J.-P., Prakash, A., Cheng, L., Chidichimo, M. P., Crate, S., Enomoto, H., Garschagen, M., Gruber, N., Harper, S., Holland, E., Rice, J., Steffen, K., and von Schuckmann, K.: Framing and Context of the Report in IPCC Special Report on the Ocean and Cryosphere in a Changing Climate [H.-O. Pörtner, D.C. Roberts, V. Masson-Delmotte, P. Zhai, M. Tignor, E. Poloczanska, K. Mintenbeck, A. Alegría, M. Nicolai, A. Okem, J. Petzold, B. Rama, N.M. Weyer (eds.)]. Cambridge University Press, Cambridge, UK and New York, NY, USA, 73-129, <https://doi.org/10.1017/9781009157964.003>, 2019.
- 425 Bates, N., Astor, Y., Church, M., Currie, K., Dore, J., Gonaález-Dávila, M., Lorenzoni, L., Muller-Karger, F., Olafsson, J., and Santacasio, M.: A Time-Series View of Changing Ocean Chemistry Due to Ocean Uptake of Anthropogenic CO<sub>2</sub> and Ocean Acidification, *Oceanography*, 27(1), 126-141, <https://doi.org/10.5670/oceanog.2014.16>, 2014.
- 430 Bittig, H. C. and Körtzinger, A.: Tackling Oxygen Optode Drift: Near-Surface and In-Air Oxygen Optode Measurements on a Float Provide an Accurate in Situ Reference, *Journal of Atmospheric and Oceanic Technology*, 32(8), 1536-1543, <https://doi.org/10.1175/JTECH-D-14-00162.1>, 2015.
- Bittig, H. C., Körtzinger, A., Neill, C., van Ooijen, E., Plant, J. N., Hahn, J., Johnson, K. S., Yang, B. and Emerson, S. R.: Oxygen Optode Sensors: Principle, Characterization, Calibration, and Application in the Ocean, *Frontiers in Marine Science*, 4:429, <https://doi.org/10.3389/fmars.2017.00429>, 2018a.
- 435 Bittig, H. C., Steinhoff, T., Claustre, H., Fiedler, B., Williams, N. L., Sauzède, R., Körtzinger, A., and Gattuso, J.-P.: An Alternative to Static Climatologies: Robust Estimation of Open Ocean CO<sub>2</sub> Variables and Nutrient Concentrations From T, S, and O<sub>2</sub> Data Using Bayesian Neural Networks, *Frontiers in Marine Science*, 5, 328, <https://doi.org/10.3389/fmars.2018.00328>, 2018b.
- Bushinsky, S. M., Takeshita, Y., and Williams, N. L.: Observing Changes in Ocean Carbonate Chemistry: Our Autonomous Future, *Current Climate Change Reports*, 5(3), 207-220, <https://doi.org/10.1007/s40641-019-00129-8>, 2019.
- 440 Carstensen, J., and Duarte, C. M. . Drivers of pH Variability in Coastal Ecosystems, *Environmental Science & Technology*, 53(8), 4020-4029, <https://doi.org/10.1021/acs.est.8b03655>, 2019.
- Carter, B. R., Feely, R. A., Williams, N. L., Dickson, A. G., Fong, M. B., and Takeshita, Y.: Updated methods for global locally interpolated estimation of alkalinity, pH, and nitrate, *Limnology and Oceanography: Methods*, 16(2), 119-131, <https://doi.org/10.1002/lom3.10232>, 2018.
- 445 Carter, B. R., Bittig, H. C., Fassbender, A. J., Sharp, J. D., Takeshita, Y., XU, Y.-Y., Álvarez, M., Wanninkhof, R., Feely, R. A., and Barbero, L.: New and updated global empirical seawater property estimation routines, *Limnology and Oceanography: Methods*, 19, 785-809, <https://doi.org/10.1002/lom3.10461>, 2021.
- De Boyer Montégut, C., Madec, G., Fischer, A.S., Lazar, A. and Iudicone, D.: Mixed layer depth over the global ocean: An examination of profile data and a profile-based climatology, *Journal of Geophysical Research*, 109, C12003. <https://doi.org/10.1029/2004JC002378>, 2004.
- 450 Dickson, A.G., C.L. Sabine, and J.R. Christian, eds.: Guide to Best Practices for Ocean CO<sub>2</sub> Measurements, PICES Special Publication 3, North Pacific Marine Science Organization, Sidney, British Columbia, 0-191, <https://doi.org/10.25607/OBP-1342>, 2007.
- Doney, S. C., Fabry, V. J., Feely, R. A., and Kleypas, J. A.: Ocean Acidification: The Other CO<sub>2</sub> Problem. *Annual Review of Marine Science*, 1(1), 169-192, <https://doi.org/10.1146/annurev.marine.010908.163834>, 2009.
- 455



- Fiedler, B., Cancouët, R., Claustre, H., Coppola, L., Cotrim da Cunha, L., Fourrier, M., Hernandez, F., Paulsen, M. and Wimart-Rousseau, C.: Report on demo mission and dissemination pathways of obtained data based on different observational platforms, EuroSea Deliverable, D7.1. EuroSea, 31 pp. [https://doi.org/10.3289/eurosea\\_d7.1,2022](https://doi.org/10.3289/eurosea_d7.1,2022).
- Friedlingstein, P., O'Sullivan, M., Jones, M.W., Andrew, R.M., Gregor, L., Hauck, J., Le Quééré, C., Luijkx, I.T., Olsen, A., Peters, G.P., Peters, W., Pongratz, J. et al.: Global Carbon Budget 2022, *Earth System Science Data*, 14(11), 4811–4900, <https://doi.org/10.5194/essd-14-4811-2022,2022>.
- Goni, G., Roemmich, D., Molinari, R., Meyers, G., Sun, C., Boyer, T., Baringer, M., Gouretski, V., DiNezio, P., Reseghetti, F., Vissa, G., Swart, S., Keeley, R., Garzoli, S., Rossby, T., Maes, C. and Reverdin, G.: The Ship of Opportunity program, *Proceedings of OceanObs'09: Sustained Ocean Observations and Information for Society*, (Vol. 2), Venice, Italy, 21-25 September 2009, Hall, J., Harrison, D.E. and Stammer, D., Eds., ESA Publication WPP-306, <https://doi.org/10.5270/OceanObs09.cwp.35,2007>.
- Gruber, N., Gloor, M., Mikaloff Fletcher, S. E., Doney, S. C., Dutkiewicz, S., Follows, M. J., Gerber, M., Jacobson, A. R., Joos, F., Lindsay, K., Menemenlis, D., Mouchet, A., Muller, S. A., Sarmiento, J. L., and Takahashi, T.: Oceanic sources, sinks, and transport of atmospheric CO<sub>2</sub>, *Global Biogeochemical Cycles*, 23(1), GB1005, <https://doi.org/10.1029/2008GB003349,2009>.
- Hunt, C., Salisbury, J. and Vandemark, D.: Contribution of non-carbonate anions to total alkalinity and overestimation of *p*CO<sub>2</sub> in new england and new brunswick rivers, *Biogeosciences*, 8 (10), 3069-3076, <https://doi.org/10.5194/bg-8-3069-2011,2011>.
- IPCC: Summary for Policymakers in *Climate Change 2021: The Physical Science Basis*. Contribution of Working Group I to the Sixth Assessment Report of the Intergovernmental Panel on Climate Change [Masson-Delmotte, V., P. Zhai, A. Pirani, S.L. Connors, C. Pe'an, S. Berger, N. Caud, Y. Chen, L. Goldfarb, M.I. Gomis, M. Huang, K. Leitzell, E. Lonnoy, J.B.R. Matthews, T.K. Maycock, T. Waterfield, O. Yelekci, R. Yu, and B. Zhou (eds.)], Cambridge University Press, Cambridge, United Kingdom and New York, NY, USA, pp. 3-32, doi:10.1017/9781009157896.001, 2021.
- Johnson, K., Wills, K., Butler, D., Johnson, W., and Wong, C.: Coulometric total carbon dioxide analysis for marine studies: maximizing the performance of an automated gas extraction system and coulometric detector, *Marine Chemistry*, 44, 167-187, [https://doi.org/10.1016/0304-4203\(93\)90201-X,1993](https://doi.org/10.1016/0304-4203(93)90201-X,1993).
- Johnson, K. S., Plant, J. N., Riser, S. C., and Gilbert, D.: Deep-Sea DuraFET: Air oxygen calibration of oxygen optodes on a profiling float array, *Journal of Atmospheric and Oceanic Technology*, 32, 2160-2172. <https://doi.org/10.1175/JTECH-D-15-0101.1,2015>.
- Johnson, K. S., Jannasch, H. W., Coletti, L. J., Elrod, V. A., Martz, T. R., Takeshita, Y., Carlson, R. J., and Connery, J. G.: Deep-Sea DuraFET: A Pressure Tolerant pH Sensor Designed for Global Sensor Networks, *Analytical Chemistry*, 88(6), 3249-3256. <https://doi.org/10.1021/acs.analchem.5b04653,2016>.
- Johnson, K. S., Plant, J. N., Coletti, L. J., Jannasch, H. W., Sakamoto, C. M., Riser, S. C., Swift, D. D., Williams, N. L., Boss, E., Haëntjens, N., Lynne D. Talley, L. D., and Sarmiento, J. L.: Biogeochemical sensor performance in the SOCCOM profiling float array, *Journal of Geophysical Research Oceans*, 122, 6416–6436. <https://doi.org/10.1002/2017JC012838,2017>.
- Johnson, K. S., Plant, J. N., and Maurer, T. L.: Processing BGC-Argo pH data at the DAC level, v1.0, *Argo data management*, <https://doi.org/10.13155/57195,2018>.
- Karstensen, J., Begler, C., Gerke, L., Handmann, P., Hans, A.-C., Lösel, C., Martens, W., Niebaum, N., Olbricht, H. D., Posern, C., Rudloff, D., Witt, R., and Wutting, P. J.: Western Subpolar North Atlantic transport variability, Cruise No. MSM94, 02. August - 06. September 2020, Emden (Germany) - Emden (Germany). In *MARIA S. MERIAN-Berichte (MSM94, pp. 1-47)*, Gutachterpanel Forschungsschiffe, [https://doi.org/10.48433/cr\\_msm94,2020](https://doi.org/10.48433/cr_msm94,2020).



- Khatiwala, S., Tanhua, T., Mikaloff Fletcher, S., Gerber, M., Doney, S. C., Graven, H. D., Gruber, N., McKinley, G. A., Murata, A., Ríos, A. F., and Sabine, C. L.: Global ocean storage of anthropogenic carbon, *Biogeosciences*, 10, 2169–2191, <https://doi.org/10.5194/bg-10-2169-2013>, 2013.
- Körtzinger, A., Rhein, M., and Mintrop, L.: Anthropogenic CO<sub>2</sub> and CFCs in the North Atlantic Ocean—A comparison of man-made tracers, *490 Geophysical Research Letters*, 26(14), 2065–2068, <https://doi.org/10.1029/1999GL900432>, 1999.
- Kwiatkowski, L., Torres, O., Bopp, L., Aumont, O., Chamberlain, M., Christian, J. R., Dunne, J. P., Gehlen, M., Ilyina, T., John, J. G., Lenton, A., Li, H., Lovenduski, N. S., Orr, J. C., Palmieri, J., Santana-Falcón, Y., Schwinger, J., Séférian, R., Stock, C. A. and Ziehn, T.: Twenty-first century ocean warming, acidification, deoxygenation, and upper-ocean nutrient and primary production decline from CMIP6 model projections, *Biogeosciences*, 17(13), 3439–3470. <https://doi.org/10.5194/bg-17-3439-2020>, 2020.
- 495 Levine, N. M., Doney, S.C., Lima, I., Wanninkhof, R., Bates, N.R. and Feely, R.A.: The impact of the North Atlantic Oscillation on the uptake and accumulation of anthropogenic CO<sub>2</sub> by North Atlantic Ocean mode waters, *Global Biogeochemical Cycles*, 25, GB3022, <https://doi.org/10.1029/2010GB003892>, 2011.
- Leseurre, C., Lo Monaco, C., Reverdin, G., Metzl, N., Fin, J., Olafsdottir, S. and Racapé, V.: Ocean carbonate system variability in the North Atlantic Subpolar surface water (1993–2017), *Biogeosciences*, 17(9), 2553–2577, <https://doi.org/10.5194/bg-17-2553-2020>, 2020.
- 500 Maurer, T. L., Plant, J. N., and Johnson, K. S: Delayed-Mode Quality Control of Oxygen, Nitrate, and pH Data on SOCCOM Biogeochemical Profiling Floats, *Frontiers in Marine Sciences*, 8, 683207, <https://doi.org/10.3389/fmars.2021.683207>, 2021.
- Newton J.A., Feely R. A., Jewett E. B., Williamson P. and Mathis J.: Global Ocean Acidification Observing Network: Requirements and Governance Plan, Second Edition, GOA-ON, [http://www.goa-on.org/docs/GOA-ON\\_plan\\_print.pdf](http://www.goa-on.org/docs/GOA-ON_plan_print.pdf), 2015.
- Olsen, A., Key, R. M., van Heuven, S., Lauvset, S. K., Velo, A., Lin, X., Schirnick, C., Kozyr, A., Tanhua, T., Hoppema, M., Jutterström, S., Steinfeldt, R., Jeansson, E., Ishii, M., Pérez, F. F. and Suzuki, T.: The Global Ocean Data Analysis Project version 2 (GLODAPv2) – an internally consistent data product for the world ocean, *Earth System Science Data*, 8(2), 297–323, <https://doi.org/10.5194/essd-8-297-2016>, 505 2016.
- Orr, J. C., Fabry, V. J., Aumont, O., Bopp, L., Doney, S. C., Feely, R. A., Gnanadesikan, A., Gruber, N., Ishida, A., Joos, F., Key, R. M., Lindsay, K., Maier-Reimer, E., Matear, R., Monfray, P., Mouchet, A., Najjar, R. G., Plattner, G.-K., Rodgers, K. B. and Yool, A.: Anthropogenic ocean acidification over the twenty-first century and its impact on calcifying organisms, *Nature*, 437(7059), 681–686. <https://doi.org/10.1038/nature04095>, 2005.
- 510 Owens, W. B. and Wong, A., P., S.: An improved calibration method for the drift of the conductivity sensor on autonomous CTD profiling floats by  $\theta$ -S climatology, *Deep Sea Research Part I: Oceanographic Research Papers*, 56(3), 450–457. <https://doi.org/10.1016/j.dsr.2008.09.008>, 2009.
- Pierrot, D., Neill, C., Sullivan, K., Castle, R., Wanninkhof, R., Lüger, H., Johannessen, T., Olsen, A., Feely, R. A. and Cosca, C. E.: Recommendations for autonomous underway pCO<sub>2</sub> measuring systems and data-reduction routines, *Deep Sea Research Part II: Tropical Studies in Oceanography*, 56(8–10), 512–522. <https://doi.org/10.1016/j.dsr2.2008.12.005>, 2009.
- Racapé, V., Zunino, P., Mercier, H., Lherminier, P., Bopp, L., Pérèz, F. F. and Gehlen, M.: Transport and storage of anthropogenic C in the North Atlantic Subpolar Ocean, *Biogeosciences*, 15, 4661–4682, <https://doi.org/10.5194/bg-15-4661-2018>, 2018.
- Ridge, S.M. and McKinley, G.A.: Advective Controls on the North Atlantic Anthropogenic Carbon Sink, *Global Biogeochemical Cycles*, 34(7), e2019GB006457, <https://doi.org/10.1029/2019GB006457>, 2020.
- 520 Russell, J., Sarmiento, J., Cullen, H., Hotinski, R., Johnson, K., Riser, S. and Talley, L.: The Southern Ocean Carbon and Climate Observations and Modeling Program (SOCCOM), *Ocean Carbon and Biogeochemistry News*, 7(2), 1–5, 2014.



- Sauzède, R., Bittig, H. C., Claustre, H., Pasqueron de Fommervault, O., Gattuso, J.-P., Legendre, L. and Johnson, K. S.: Estimates of Water-Column Nutrient Concentrations and Carbonate System Parameters in the Global Ocean: A Novel Approach Based on Neural Networks, *Frontiers in Marine Science*, 4, 128, <https://doi.org/10.3389/fmars.2017.00128>, 2017.
- 525 Sabine, C. L., Feely, R. A., Gruber, N., Key, R. M., Lee, K., Bullister, J. L., Wanninkhof, R., Wong, C. S., Wallace, D. W. R., Tilbrook, B., Millero, F. J., Peng, T.-H., Kozyr, A., Ono, T., and Rios, A. F.: The oceanic sink for anthropogenic CO<sub>2</sub>, *Science*, 305(5682), 367-371, <https://doi.org/10.1126/science.1097403>, 2004.
- Sabine, C. L., Hankin, S., Koyuk, H., Bakker, D. C. E., Pfeil, B., Olsen, A., Metzl, N., Kozyr, A., Fassbender, A., Manke, A., Malczyk, J., Akl, J. et al.: Surface Ocean CO<sub>2</sub> Atlas (SOCAT) gridded data products, *Earth System Science Data*, 5(1), 145-153, <https://doi.org/10.5194/essd-530-5-145-2013>, 2013.
- Schmechtig, C., Thierry, V. and Team, T. B. A.: Argo quality control manual for biogeochemical data (1.0), Bio-Argo group, <https://doi.org/10.13155/40879>, 2016.
- Takeshita, Y., Johnson, K. S., Coletti, L. J., Jannasch, H. W., Walz, P. M. and Warren, J. K.: Assessment of pH dependent errors in spectrophotometric pH measurements of seawater, *Marine Chemistry*, 223, 103801, <https://doi.org/10.1016/j.marchem.2020.103801>, 2020.
- 535 Soetaert, K., Hofmann, A., Middelburg, J., Meysman, F. and Greenwood, J.: The effect of biogeochemical processes on pH, *Marine Chemistry*, 105(1), 30-51, <https://doi.org/10.1016/j.marchem.2006.12.012>, 2007.
- Tanhua, T., McCurdy, A., Fischer, A., Appeltans, W., Bax, N., Currie, K., DeYoung, B., Dunn, D., Heslop, E., Glover, L. K., Gunn, J., Hill, K., Ishii, M., Legler, D., Lindstrom, E., Miloslavich, P., Moltmann, T., Nolan, G., Palacz, A. and Wilkin, J.: What We Have Learned From the Framework for Ocean Observing: Evolution of the Global Ocean Observing System, *Frontiers in Marine Science*, 6, <https://www.frontiersin.org/article/10.3389/fmars.2019.00471>, 2019.
- 540 van Heuven, S., Pierrot, D., Rae, J. W. B., Lewis, E. and Wallace, D. W. R.: MATLAB Program Developed for CO<sub>2</sub> System Calculations. ORNL/CDIAC-105b, Carbon Dioxide Information Analysis Center, Oak Ridge National Laboratory, U.S. Department of Energy, Oak Ridge, Tennessee, [https://doi.org/10.3334/CDIAC/otg.CO2SYS\\_MATLAB\\_v1.1](https://doi.org/10.3334/CDIAC/otg.CO2SYS_MATLAB_v1.1), 2011.
- Watson, A. J., Schuster, U., Bakker, D. C., Bates, N. R., Corbière, A., González-Dávila, M., Friedrich, T., Hauck, J., Heinze, C., Johannessen, T., Körtzinger, A., Metzl, N., Olafsson, J., Olsen, A., Oschlies, A., Padin, X. A., Pfeil, B., Santana-Casiano, J. M., Steinhoff, T., Telszewski, M., Rios, A. F., Wallace, D. W. and Wanninkhof, R.: Tracking the variable North Atlantic sink for atmospheric CO<sub>2</sub>, *Science*, 326(5958), 1391-3, <https://doi.org/10.1126/science.1177394>, 2009.
- Wanninkhof, R., Bakker, D., Bates, N., Olsen, A., Steinhoff, T. and Sutton, A.: Incorporation of Alternative Sensors in the SOCAT Database and Adjustments to Dataset Quality Control Flags, <http://cdiac.ornl.gov/oceans/Recommendationnewsensors.pdf>. Carbon Dioxide Information Analysis Center, Oak Ridge National Laboratory, US Department of Energy, Oak Ridge, Tennessee, [https://doi.org/10.3334/CDIAC/OTG.SOCAT\\_ADQCF](https://doi.org/10.3334/CDIAC/OTG.SOCAT_ADQCF), 2013.
- 545 Whitt, C., Pearlman, J., Polagy, B., Caimi, F., Muller-Karger, F., Copping, A., Spence, H., Madhusudhana, S., Kirkwood, W., Grosjean, L., Fiaz, B. M., Singh, S., Singh, S., Manalang, D., Gupta, A. S., Maguer, A., Buck, J. J. H., Marouchos, A., Atmanand, M. A. and Khalsa, S. J.: Future Vision for Autonomous Ocean Observations, *Frontiers in Marine Science*, 7, <https://doi.org/10.3389/fmars.2020.00697>, 2020.
- Williams, N. L., Juranek, L. W., Johnson, K. S., Feely, R. A., Riser, S. C., Talley, L. D., Russell, J. L., Sarmiento, J. L. and Wanninkhof, R.: Empirical algorithms to estimate water column pH in the Southern Ocean, *Geophysical Research Letters*, 43(7), 3415-3422, <https://doi.org/10.1002/2016GL068539>, 2016.
- 550 Wong, A., Keeley, R., Carval, T. and Team, A. D. M.: Argo Quality Control Manual for CTD and Trajectory Data (3.6) [Pdf], Ifremer, <https://doi.org/10.13155/33951>, 2022.

<https://doi.org/10.5194/bg-2023-76>  
Preprint. Discussion started: 22 May 2023  
© Author(s) 2023. CC BY 4.0 License.



Zeebe, R. E. and Wolf-Gladrow, D.: CO<sub>2</sub> in seawater : equilibrium, kinetics, isotopes, Elsevier Oceanography Book Series, 65, 346 pp, Amsterdam, ISBN:0444 – 50946 – 1, 2001.